Cell, Vol. 100, 209–219, January 21, 2000, Copyright ©2000 by Cell Press

Directed Actin Polymerization Is the Driving Force for Epithelial Cell–Cell Adhesion

Valeri Vasioukhin, Christoph Bauer, Mei Yin, and Elaine Fuchs*
Department of Molecular Genetics and Cell Biology
Howard Hughes Medical Institute
The University of Chicago
Chicago, Illinois 60637

Summary

We have found that epithelial cells engage in a process of cadherin-mediated intercellular adhesion that utilizes calcium and actin polymerization in unexpected ways. Calcium stimulates filopodia, which penetrate and embed into neighboring cells. E-cadherin complexes cluster at filopodia tips, generating a two-rowed zipper of embedded puncta. Opposing cell surfaces are clamped by desmosomes, while vinculin, zyxin, VASP, and Mena are recruited to adhesion zippers by a mechanism that requires α-catenin. Actin reorganizes and polymerizes to merge puncta into a single row and seal cell borders. In keratinocytes either null for α-catenin or blocked in VASP/Mena function, filopodia embed, but actin reorganization/polymerization is prevented, and membranes cannot seal. Taken together, a dynamic mechanism for intercellular adhesion is unveiled involving calcium-activated filopodia penetration and VASP/Mena-dependent actin reorganization/polymerization.

Introduction

Cell–cell adhesion is critical for tissues and organs. Adherens junctions (AJs) are intercellular structures prominent in epithelia and neurons (Nose et al., 1988; Geiger et al., 1992; Drubin and Nelson, 1996; Gumbiner, 1996). The electron dense transmembrane core of the AJ is composed of cadherins, of which E-cadherin is the epithelial prototype. Abundant in epithelia and heart muscle are specialized cadherins called desmogleins and desmocollins, which form less dynamic and more robust structures called desmosomes (Kowalczyk et al., 1999). The extracellular domains of cadherins change conformation in response to calcium, engaging in homotypic interactions to specify cell–cell connections (Nose et al., 1988; Shapiro et al., 1995). This feature is thought to account fully for the requirement of calcium in intercellular adhesion.

Adhesive properties of cadherins depend on their cytoplasmic domain. For desmosomal cadherins, this domain binds plakoglobin and desmoplakin, and indirectly associates with intermediate filaments (IFs; Kowalczyk et al., 1999). In contrast, E-cadherin's cytoplasmic domain binds β-catenin, which in turn binds α-catenin. While β-catenin plays a regulatory role in adhesion, α-catenin links the actin cytoskeleton to AJs (Drubin and Nelson, 1996; Gumbiner, 1996).

α-catenin associates with several other actin-binding proteins, including a cousin, vinculin, and α-actinin, neither of which is exclusive to AJs (Geiger et al., 1992; Knudsen et al., 1995; Hazan et al., 1997). The possibility has been raised that vinculin might share partial functional redundancy with α-catenin (Hazan et al., 1997). Several other proteins can reside at cell–cell borders, but it is not known whether they associate specifically with AJs. Among these is VASP, a protein that normally localizes to focal contacts, lamellipodia, and some bacterial pathogens that pirate actin polymerization for generating virulent movement (Reinhard et al., 1992, 1999; Laurent et al., 1999).

The actin cytoskeleton is central to intercellular adhesion. E-cadherin, α-catenin, and β-catenin coassemble into Triton X-100 insoluble structures with kinetics that parallel those of AJ formation (Angres et al., 1996). In calcium-activated, kidney epithelial cell lines (MDCK and NRK), AJ antibodies first reveal these structures as dots or "puncta" at sites of cell–cell contact (Yonemura et al., 1995; Adams et al., 1996, 1998). Although it is not clear how a punctum forms, how its size is constrained, or how its lifetime is controlled, new puncta are added as the region of intercellular contact grows. Time-lapse imaging and electron microscopy suggest that puncta are spatially coincident with membrane attachment sites for actin filaments that branch from the cortical actin cytoskeleton. Over time, the actin cytoskeleton remodels, concomitant with changes in puncta distribution (Adams et al., 1998). The function and mechanism underlying this rearrangement remain to be elucidated. However, several reports suggest that small GTPases of the Rho family may be involved since (a) MDCK cells expressing a constitutively active Cdc42 accumulate more actin filaments at sites of intercellular adhesion (Kodama et al., 1999) and (b) dominant-negative Rho and Rac interfere with actin reorganization and intercellular adhesion in epithelial cells (Braga et al., 1997, 1999).

A number of important issues remain unsettled. Our present understanding of AJ formation lacks satisfactory mechanisms to explain the interesting formation of puncta and the actin dynamics associated with intercellular adhesion. α-catenin's ability to link E-cadherin to the cortical cytoskeleton does not on its own explain the involvement of small GTPases, nor is this linkage sufficient to account for the reorganization of actin that occurs as epithelial sheets form. Intrigued by these quandaries, we wondered whether the process may have been partially obscured by conventional use of established epithelial cell lines that are generally poorly adherent and not perfectly contact inhibited. Any partial overlap of passively contacting cell membranes could significantly affect the mechanism of intercellular adhesion, as could major alterations in actin cytoskeleton long known to exist in transformed cells (Geiger et al., 1992). We therefore investigated AJ formation in primary mouse keratinocytes, which has led us to novel insights.

When perfectly contact-inhibited primary cells are

*To whom correspondence should be addressed (e-mail: nliptak@midway.uchicago.edu).

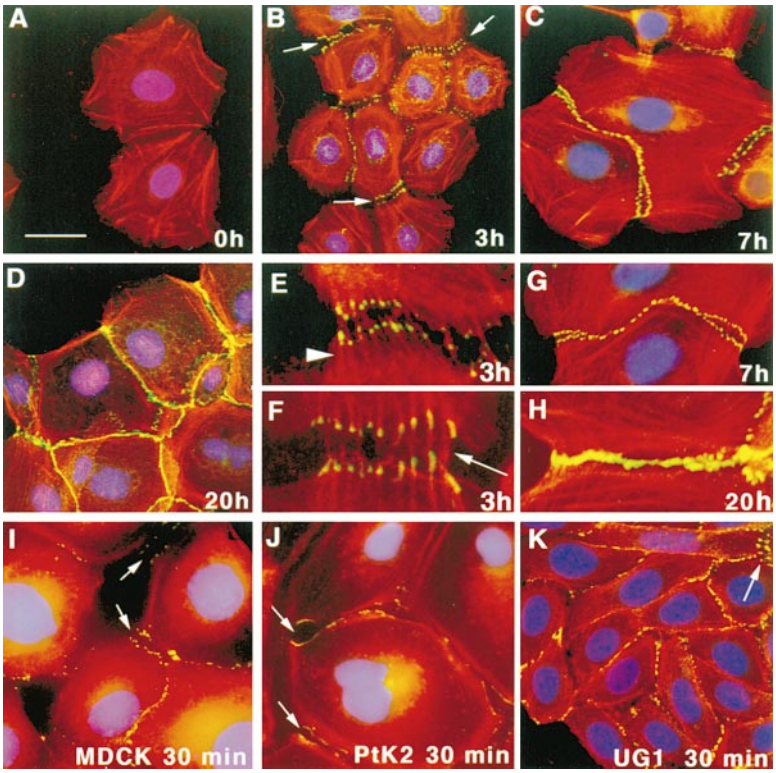

Figure 1. Formation of Adhesion Zippers: A Prelude to AJs

Primary epidermal keratinocytes (A–H) or established lines (I–K) were cultured for 24 hr, and formation of cadherin-mediated junctions was induced by calcium for the times indicated on each frame. Cells were then processed for indirect immunofluorescence using phalloidin to decorate F-actin (red) and anti-E-cadherin (green). Arrows in B denote adhesion zippers, composed of two rows of anti-E-cadherin stained puncta, separated by thin phalloidin-staining fibers (higher magnification in E and F). Arrowhead in (E) denotes cytoplasmic radial actin fibers emanating from puncta; arrow in (F) denotes actin fibers between puncta. By 7 hr, the central segments of zippers merged into a single row (C; higher magnification in G). Note: Adhesion zippers in established lines were ~10× fewer than in primary cultures. Bar in (A) represents 30 μm for (B), (D), (I), (J), and (K); 20 μm for (A); 15 μm for (C); 10 μm for (E)–(H).

stimulated, they form intercellular junctions by an active and dynamic process, driven by actin filament polymerization. This remarkable mechanism involves the calcium-activated production of filopodia, which penetrate and embed into neighboring cells. The physical force of drawing two opposing membranes together, maximized at the tip of each embedded filopodium, catalyzes clustering of AJ proteins, which include not only E-cadherin and catenins, but also VASP, Mena (related to VASP), vinculin, and zyxin. We show that this process yields two rows of embedded puncta, whose stabilization depends upon α-catenin, VASP/Mena, and actin polymerization and reorganization. This mechanism provides the force necessary to actively bring epithelial cells together and seal them into continuous sheets.

Results

The Adhesion Zipper as an Intermediate Step in AJ Formation

To examine the kinetics of AJ assembly, we first plated freshly isolated, primary mouse epidermal keratinocytes at 50% confluence on a collagen, fibronectin, and polylysine substratum, conditions where cells are not already tightly packed. When cultured in low calcium medium for 24 hr ($t = 0$), these cells formed a robust network of actin stress fibers, which bound rhodamine-labeled phalloidin (Figure 1A). No staining was observed with AJ antibodies, consistent with the fact that under low calcium conditions, neither AJs nor desmosomes form.

Within 3 hr after the switch to high calcium, anti-E-cadherin labeled two distinct and highly organized rows of puncta at sites of intercellular contact (Figures 1B, 1E, and 1F). This contrasted with disorganized puncta noted in established kidney epithelial lines (Yonemura et al., 1995; Adams et al., 1996, 1998). Each dot of anti-E-cadherin staining was aligned with an identically positioned dot in the opposing row. As expected, puncta also stained with anti-α-catenin and anti-β-catenin, but not desmosome-specific markers (not shown). Double rows of puncta were observed irrespective of whether keratinocytes were switched from low to high calcium or placed in high calcium from the start, suggesting that the structure represented an intermediate step in adhesion, rather than a reaction to calcium.

Prominent bundles of actin filaments radiated internally from puncta, (arrowhead in Figure 1E), and actin fibers existed between opposing puncta (arrow in Figure 1F). After 7 hr, the number of puncta at zippers had increased by several fold, and puncta at the centers had often merged to form a single row (Figures 1C and 1G). After 20 hr, puncta had fused to form a continuous line (Figures 1D and 1H).

We propose to call the two-rowed puncta structure an "adhesion zipper," and later, we reveal its ultrastructure. Notably, we observed adhesion zippers in both MDCK and PtK2 cells (Figures 1I and 1J). While puncta were plentiful in these cultures, adhesion was accelerated and zippers were often masked by puncta disorganization. Moreover, in contrast to primary keratinocytes, which were flat and displayed abundant stress fibers, MDCK and PtK2 cells were relatively round, with few stress fibers.

The differences in actin organization and AJ formation seemed rooted in the number of passages that cells were subjected to in culture. Thus, after 15 passages, surviving immortalized keratinocytes behaved more similarly to MDCK and PtK2 cells in their roundness, actin cytoskeleton, and rarity of zippers (Figure 1K). Based on these observations, adhesion zippers appear

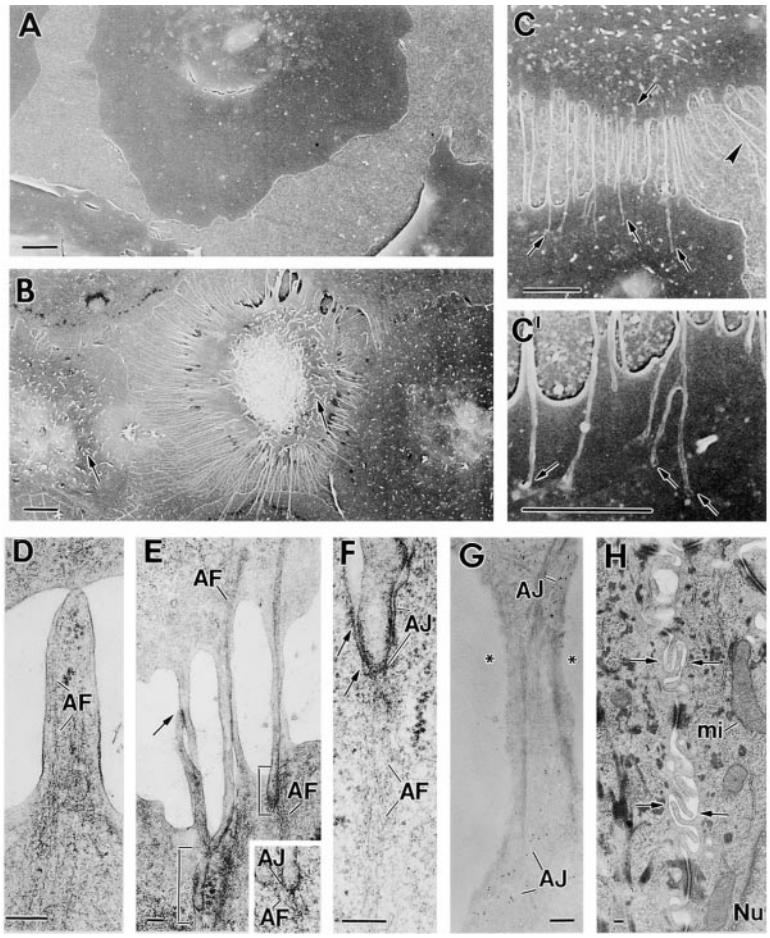

Figure 2. Ultrastructural Analysis of Adhesion Zippers

Primary keratinocytes were cultured, and at t = 0 (A) or 3 hr (B–G) following the calcium switch, cells were fixed and processed for scanning (A–C′), conventional (D–F, H), or immuno (G) electron microscopy. Arrows in (B) denote microspikes. Arrows in (C) and (C′) denote filopodia embedded into neighboring keratinocytes; arrowheads in (C) denote branched, disorganized filopodia in regions devoid of contact. Arrows in (E) denote antiparallel pairs of filopodia making contact with and embedding into the opposing plasma membrane (brackets). Inset to (E) and (F) shows electron dense AJs at filopodia tip anchored to actin filament bundles (AF). Arrows in (F) denote membrane of filopodial pocket. (G) Tips of a filopodia pair labeled with α-catenin antibodies. Asterisks denote regions where opposing membranes are unsealed. (H) Filopodial pairs (double arrows) at sites of intercellular contact in mouse skin epidermis. Bars represent 5 μm for (A)–(C) and (H); 200 nm for (D)–(G).

to be a natural intermediate in adhesion, but become aberrant during immortalization or transformation.

Calcium Activates Formation and Propulsion of Filopodia into Neighboring Cells to Initiate AJ Formation

To probe more deeply into the structure of adhesion zippers, we repeated the calcium switch experiments, this time processing cells for both scanning and transmission electron microscopy. At low calcium, cells were well spread, round, and extended only a few random processes (Figure 2A). In high calcium, cell surfaces changed markedly, exhibiting membrane ruffling over nuclei and numerous microspikes (Figure 2B). Most prominent were long filopodial processes making contact with substratum. Although thin cellular processes have been noted previously in regions where epithelial cells make contact, neither their abundance nor their stimulation by calcium have been reported (Yonemura et al., 1995). Our findings were interesting in light of correlations between calcium and filopodial formation in other cells, particularly neurons (Lau et al., 1999 and references therein).

After the calcium switch, overall filopodia numbers were elevated, but the greatest number were always at intercellular contacts (Figure 2C). Intriguingly, filopodia making contact with neighboring cells appeared to physically embed into the neighboring cell membrane (Figure 2C′ and arrows in Figure 2C). Filopodia not making contact were often branched and randomly oriented (arrowheads in Figure 2C).

Each filopodium was packed with cytoskeleton that was largely if not solely composed of actin filaments (Figure 2D). While some filopodia made contact with neighboring cell surfaces (example in Figure 2D), others contacted opposing filopodia (arrow in Figure 2E). Upon contact, opposing filopodia seemed to slide as antiparallel dimers along one another until they embedded, becoming encased by a membrane pocket (Figure 2F). At embedded filopodial tips, electron dense structures resembling AJs formed (Figures 2E and 2F). These structures labeled with AJ antibodies, confirming their identity (Figure 2G). Membranes flanking each opposing filopodia pair were still separated, creating alternating zones of gaps and contacts.

The average depth of projectiles at the center of a 3 hr zipper was 1.1 μM ± 0.2 μM. This coincided quite well with the positioning of cortical cytoskeleton relative to the cell membrane. The pairing of opposing filopodia, the concentration of AJs at each tip, and the approximate distance of filopodia penetration also agreed well with the distances and positioning of two opposing rows of puncta (see Figure 1). Thus, the phalloidin staining between two puncta rows corresponded to the actin-filled filopodial extensions spanning two contacting cells. Taken together, these data reveal the structure

and origin of adhesion zippers and uncover a novel role for calcium in adhesion.

While cell culture enabled us to study how filopodia form during intercellular adhesion, the existence of filopodial projectiles is not unique to cultured keratinocytes. Epidermal cells in mouse skin display abundant projectiles, which often pair in a fashion resembling that in culture (Figure 2H). Thus, it seems likely that the process of filopodia extension and pairing is a characteristic of intercellular adhesion in vivo as well as in vitro.

Filopodia Tips/Puncta Serve as Sites for Actin Polymerization and for Recruitment of Vinculin, Zyxin, VASP, and Mena

As predicted from prior studies on puncta formation (Adams et al., 1996, 1998), the ability to form adhesion zippers was dependent on actin cytoskeleton. Zippers did not assemble in the presence of cytochalasin D, a potent inhibitor of actin polymerization (Figures 3A–3D). Additionally, while some E-cadherin still localized at intercellular contacts 20 hr after the calcium switch in cytochalasin D, epithelial sheets did not form, and large gaps were seen even in closely positioned cells (Figure 3D).

The intricate link between actin filaments and adhesion zippers was evident by immunofluorescence microscopy, where each punctum associated with a cellular actin fiber (Figure 1E). This was confirmed by ultrastructure, where a bundle of actin filaments emanated from the base of each filopodial pocket (Figure 2F). To explore how these actin fibers form, we activated intercellular adhesion and incubated permeabilized keratinocytes briefly with rhodamine actin. Rhodamine actin concentrated at puncta (Figures 3E and 3F). Colabeling with FITC-phalloidin verified that rhodamine actin represented only a small fraction of total actin and that actin fibers were associated with each rhodamine-labeled dot. Thus, puncta are sites of active actin polymerization.

To a lesser extent, rhodamine actin incorporated at free filopodia tips (arrows in Figures 3E and 3F). Therefore, actin polymerization at puncta occurred predominantly at the cytoplasmic side, where actin fibers connected to each filopodia pocket. Further experiments below provide additional evidence in support of this notion.

We next examined whether molecular catalysts for actin dynamics might be involved in actin organization at zippers. The two major orchestrators known are N-WASP and relatives, which bind Cdc42 and Arp2/3 complexes to nucleate actin polymerization (Rohatgi et al., 1999), and VASP/Ena family members, which bind either zyxin/vinculin (mammalian cells) or ActA (*Lysteria*) to reorganize existing actin filaments and stimulate polymerization (Laurent et al., 1999). Cdc42 and VASP both have been detected at sites of epithelial contacts (Kuroda et al., 1997; Stoffler et al., 1998; Reinhard et al., 1999), although it is unknown whether they are specifically involved in AJs. We took advantage of the specificity of puncta to assess which if any of the major candidates might stimulate or direct actin polymerization at newly formed AJs.

Anti-N-WASP antibodies did not preferentially label

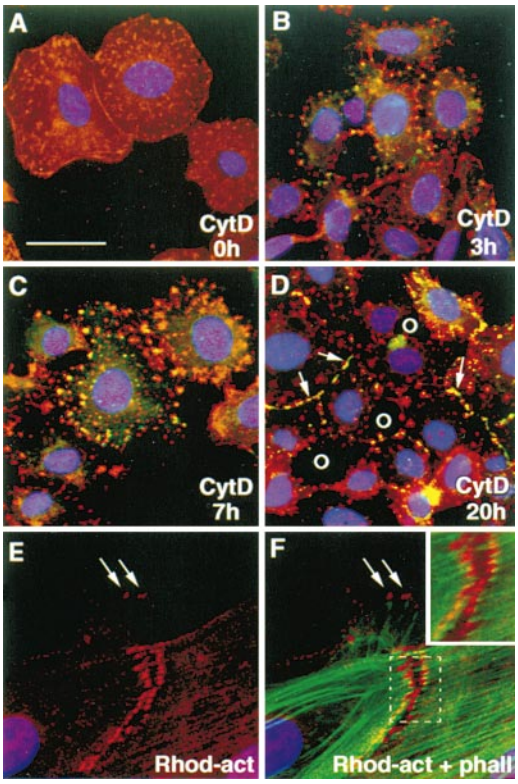

Figure 3. Actin Polymerization at Adhesion Zippers

(A–D) At 24 hr after plating, keratinocytes were switched to high calcium medium containing 2 μM cytochalasin D (Calbiochem, La Jolla, CA) for times indicated, and then processed for immunofluorescence microscopy using anti-E-cadherin (green) and phalloidin (red). Adhesion zippers did not form, but some cadherin localized to cell borders at 20 hr (arrows in D). Gaps between cells (open circles in D) indicated that cells did not seal to form sheets.

(E and F) At 24 hr after plating, keratinocytes were switched to high calcium medium for 3 hr, and then permeabilized briefly with saponin and exposed to 0.5 μM rhodamine-labeled actin for 1, 3, 5, and 10 min (Symons and Mitchison, 1991). Cells were fixed with 4% formaldehyde and colabeled with FITC-phalloidin. Shown are single and double labeling of same intercellular junction (t = 3 min). Note incorporation of rhodamine actin at adhesion zipper (area in dotted white box is magnified in inset). Note weaker labeling at membrane edges and free filopodial tips (arrows).

Bar in (A) represents 40 μm in (A)–(D), 10 μm in (E) and (F).

zippers or mature AJs (not shown). In contrast, antibodies against vinculin, zyxin, VASP, and Mena labeled not only focal contacts (as expected) but also puncta (Figures 4A–4E). While vinculin was already a well-known AJ component (Geiger et al., 1992; Hazan et al., 1997), our results added VASP, zyxin, and Mena to this structure. Recent reviews postulate that zyxin could be a component of AJs through its ability to bind to α-actinin (Bershadsky and Geiger, 1998). While both anti-α-actinin and anti-zyxin labeled puncta, α-actinin also associated with radial actin fibers, consistent with its actin-bundling properties (Figure 4F). This pattern was distinct from that of anti-zyxin.

Our findings placed the VASP, zyxin, Mena, and vinculin at puncta, a specific stage in epithelial sheet formation. Since these proteins have been localized to other

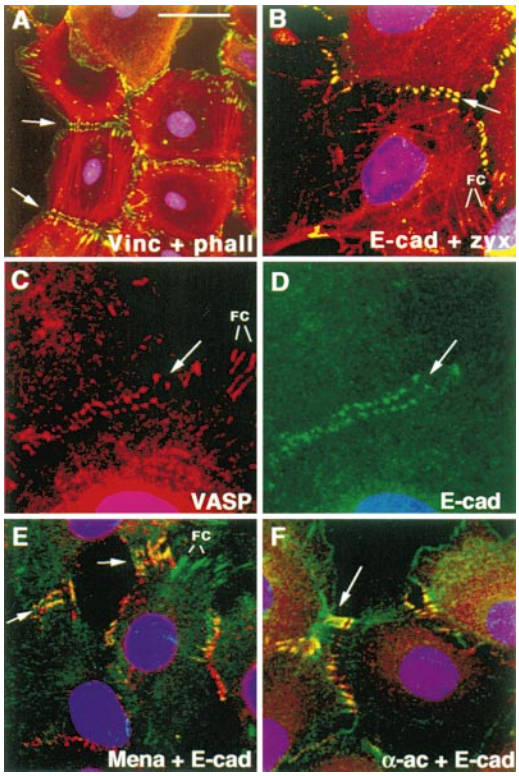

Figure 4. Vinculin, Zyxin, VASP, and Mena Are Components of Adhesion Zippers

Indirect immunofluorescence microscopy was conducted on primary keratinocytes exposed to calcium for 3 hr. Antibodies are indicated on each frame: green, first; red, second. Abbreviations for antibodies are: E-cad, E-cadherin; Vinc, vinculin; phall, phalloidin; zyx, zyxin; α-ac, α-actinin. Arrow in (F) denotes α-actinin on radial actin fibers extending from adhesion zippers. Arrows in other frames denote adhesion zippers. Note that antibodies to vinculin, zyxin, VASP, and Mena labeled focal contacts (FC) as well as zippers. Bar represents 40 μm in (A), (E), and (F); 20 μm in (B); 10 μm in (C) and (D).

cellular regions where actin reorganization and polymerization is required (Machesky and Insall, 1999), a potential mechanism emerged to explain not only the incorporation of rhodamine actin at puncta, but also the organized bundles of actin filaments emanating from puncta.

α-Catenin Is Essential for VASP/Mena Localization and for Adhesion Zipper and Epithelial Sheet Formation

Since anti-VASP and anti-Mena labeling was weak at free filopodia tips, the concentration of VASP and Mena at zippers is likely to reside at cytoplasmic sites where filopodia embed and where radial actin fibers emanate. VASP and Mena directly bind vinculin and zyxin, and vinculin binds α-catenin, leading us to posit that α-catenin might recruit VASP/Mena to puncta. To obtain primary α-catenin null cells necessary to test this hypothesis, we used conditional knockout technology to ablate the E-α-catenin gene in the epidermis of mice, and then prepared keratinocyte cultures from their skin.

Primary α-catenin null keratinocytes organized actin differently than wild type. In low calcium, mutant cells displayed fewer stress fibers but a rather prominent actin ring at the periphery (Figure 5A). In high calcium, these cells failed to form adhesion zippers even after 7 hr (Figures 5B and 5C). By 20 hr, anti-E-cadherin labeled a few contacting keratinocytes (Figure 5D). However, zippers did not form, and even the few single rows of puncta were discontinuous. Furthermore, while actin fibers were detected near sites of anti-E-cadherin staining, they were not organized properly (inset to Figure 5D).

As expected, the low level of anti-E-cadherin at intercellular borders of α-catenin null cultures at t = 20 hr was accompanied by anti-β-catenin colabeling (not shown), but not anti-α-catenin staining (Figure 5E). Other AJ proteins failed to localize to puncta (Figures 5F and 5G). Curiously, while zyxin and vinculin remained at focal contacts in α-catenin null cultures (Figure 5F), Mena and VASP appeared diffuse throughout the cells (Figure 5G). While future studies will be needed to fully understand the significance of this finding, our results underscored a role for α-catenin in localizing vinculin, zyxin, VASP, and Mena to puncta and in stabilizing these structures.

To explore further the role of α-catenin in puncta formation and actin reorganization, we prepared cultures containing a mixture of α-catenin null and wild-type keratinocytes. Null keratinocytes were identified by the presence of Cre-recombinase in their nuclei. Under conditions where one keratinocyte was null for α-catenin and the other wild-type, zippers still formed (Figure 5H). However, in the cell lacking α-catenin, actin fibers at puncta were not radially organized, thus establishing a role for α-catenin in this rearrangement. Overall, these data demonstrate that α-catenin is not required for filopodial formation and propulsion, but that cytoskeletal anchorage on one side of an AJ is essential for puncta formation and stabilization. Notably, radial reorganization of actin fibers was not essential for puncta stabilization, since we observed two, rather than one, rows of puncta in mixed cultures.

Altering VASP Function Perturbs Adhesion Zipper and Epithelial Sheet Formation In Vitro and In Vivo

To assess the role that VASP and Mena might play in intercellular adhesion, we perturbed VASP/Mena function in keratinocytes. The Ena/VASP family members share a tripartite structure, consisting of (a) an N-terminal segment (EVH1), necessary for interaction with ActA, vinculin, and zyxin, (b) a central core capable of binding profilin, and (c) a C-terminal segment (EVH2) for tetramerization and binding to filamentous actin (Niebuhr et al., 1997; Beckerle, 1998; Huttelmaier et al., 1998; Bachmann et al., 1999). This information has been used to devise strategies to disrupt or perturb VASP/Mena/ActA function in fibroblasts.

For our studies, we used three different agents. To compete for VASP/Mena binding to vinculin/zyxin, a peptide, CFEFPPPPTDE (Southwick and Purich, 1994; Niebuhr et al., 1997), was microinjected into primary keratinocytes at intracellular concentrations of 100 nM to 1 μM. We also engineered expression vectors for either wild-type or dominant-negative mutant forms of VASP, linked to green fluorescent protein (GFP). One of

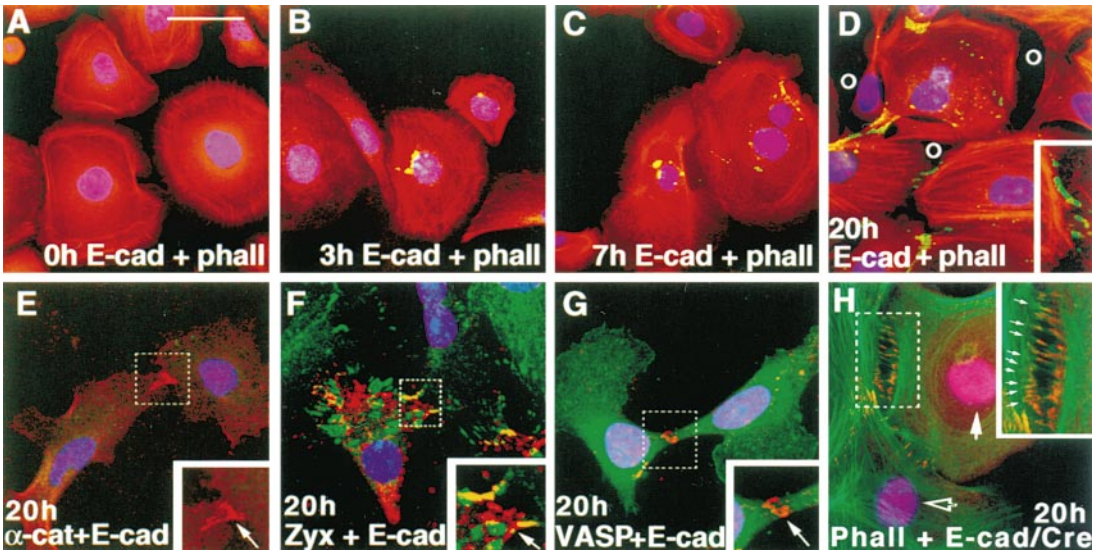

Figure 5. Consequences to Adhesion Zipper and Epithelial Sheet Formation When Both or One of Two Opposing Keratinocytes Is Null for α-Catenin

At 24 hr after plating, primary α-catenin null keratinocytes (A–G) or a mixture of α-catenin null and wild-type keratinocytes (H) were switched to high calcium medium for times indicated and then processed for immunofluorescence microscopy. Antibodies are indicated on each frame: green, first; red, second. Note that α-catenin null keratinocytes display few stress fibers and fail to form adhesion zippers, but do show some anti-E-cadherin (E-cad) staining at cell interfaces by 20 hr (D and arrows in insets to E–G). Open circles denote gaps between cells. Note: in the absence of α-catenin, only E-cadherin (shown) and β-catenin (not shown) localized in a few spots at cell–cell borders; zyxin, vinculin (not shown), Mena (not shown), and VASP no longer localized to these sites (compare data in (E)–(G) with that of wild-type keratinocytes in Figure 4). (H) The cell in the upper right lacks α-catenin as judged by nuclear labeling of anti-Cre recombinase (red nucleus, arrowhead, versus wild-type nucleus, open arrowhead). With its wild-type neighbors, the cell made double-rowed puncta, which were normal except for a lack of radial actin fibers (arrows) emanating from the puncta row within the mutant cell (inset). Regions in white dotted boxes are magnified as insets. Bar represents 40 μm for (A)–(G); 35 μm for (H).

these encoded the EVH1 domain (Niebuhr et al., 1997), while the other encoded the tetramerization domain (TD) of EVH2 (Bachmann et al., 1999). In all assays, EVH1 peptide, EVH1-GFP, and TD-GFP behaved similarly. Since TD-GFP displayed the most potent inhibition, we present these data.

Full-length VASP-GFP localized to adhesion zippers and cell–cell borders with no obvious deleterious effects (Figures 6A–6D). This was true in the majority (>90%) of transfected cells, even those that fluoresced highly with GFP (examples shown). In contrast, TD-GFP interfered with formation of adhesion zippers and epithelial sheets (Figures 6E–6H). In transfected cells subjected to a calcium switch, VASP and Mena no longer localized to cell borders (inset in Figure 6H), and wherever two transfected cells made contact, zippers had not formed by 3 hr (Figures 6E and 6F), and membrane sealing was often not seen after 20 hr (Figures 6G and 6H). However, when TD-GFP transfected cells neighbored an untransfected cell, both adhesion zippers and membrane sealing were observed. In these cases, only the wild-type cell displayed radial actin fibers (inset to Figure 6E). From these data, we conclude that VASP and Mena are required for the actin dynamics necessary to seal membranes into epithelial sheets.

To assess whether VASP function is essential for intercellular adhesion in vivo, we engineered transgenic mice expressing TD-GFP under the control of the keratin 14 promoter and enhancer, active in the innermost (basal) layer of the epidermis. The skin of K14 TD-GFP transgenic newborn animals blistered, and histological analysis revealed gross abnormalities in intercellular adhesion (Figures 6I and 6J). Most notably, very little contact existed between many of the basal cells (inset to Figure 6J), which normally possess few desmosomes and rely on adherens junctions for intercellular adhesion. Despite this major defect, adhesion of the basal cells to underlying basement membrane was seemingly unperturbed. Basal cell-substratum contacts are mediated largely through integrin-based hemidesmosomes, and disruption of VASP did not appear to affect these junctions.

While Mena and VASP localization was disrupted, E-cadherin still localized to intercellular borders (Figures 6K and 6L). Intriguingly, double lines of anti-E-cadherin labeling were often seen between cells (arrowheads in Figure 6L). While the relation of these double lines to adhesion zippers remains to be evaluated, membrane sealing and sheet formation was clearly inhibited (Figure 6J). Taken together, our findings illuminate an essential role for VASP in intercellular adhesion in vivo as well as in vitro.

How Actin Polymerization Might Be Utilized: Ultrastructural Analysis of the Fate of Embedded Puncta

The contact achieved by formation of embedded filopodia and AJs frequently resulted in desmosome assembly at flanking sites (Figures 7A–7C). This suggested

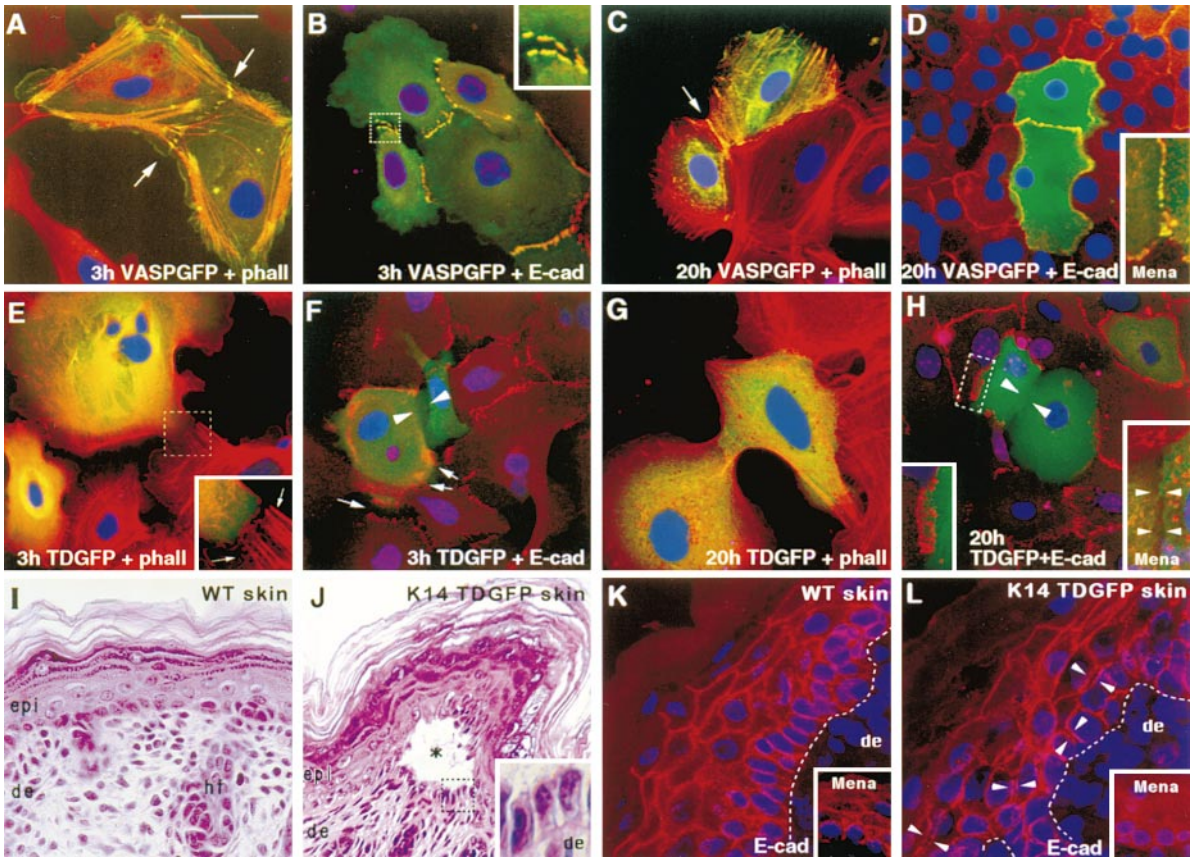

Figure 6. Disruption of VASP Function In Vitro and In Vivo Interferes with Epithelial Sheet Formation

(A–H) At 24 hr after plating, keratinocytes were transfected with expression vectors encoding VASP-GFP or TD-GFP, and 24 hr later, calcium was added for times indicated. Cells were then processed for immunofluorescence microscopy with phalloidin (red), anti-E-cadherin (red), or anti-Mena (red; insets to D, H, K, and L). VASP was visualized by the green autofluorescence of the GFP tag. (Inset to E) Arrows denote radial actin fibers in an untransfected cell, but not in the adjacent transfected cell. Areas in dotted boxes are magnified as insets. Arrows in main frames denote adhesion zippers and/or mature junctions; opposing arrowheads denote borders between two transfected cells where zippers and/or mature junctions fail to form. White dotted box in (H) denotes immature junction.

(I–L) Skins from WT (I and K) or K14 TD-GFP (J and L) transgenic mouse stained with hematoxylin and eosin (I and J) or antibodies against E-cadherin (red) (K and L).

Bar represents 35 μm for (A), (B), (E), and (G); 25 μm for (C), (D), (F), (H); 100 μm for (I) and (J); 50 μm for (K) and (L). Asterisk denotes separation between basal and suprabasal epidermal layers. Arrowheads in (L) denote double lines of anti-E-cadherin staining. Epi, epidermis; de, dermis; hf, hair follicle.

that desmosomes might passively serve to keep cell membranes together once filopodial penetration had actively brought them together. Moreover, since filopodia excluded keratin IFs, natural zones for AJ formation were interdigitated with zones permitting desmosome assembly and IF anchorage (Figures 7D and 7E). This phenomenon explains why desmosomes and AJs often alternate in epithelial sheets.

In regions abundant with desmosomes, empty filopodial membrane pockets were detected (brackets in Figure 7B). A few filopodia appeared to be "utilized" for subsequent stages of adhesion, as nascent desmosomes sometimes linked membranes between a partially relaxed pocket and its filopodium (Figure 7B). Thus, while some filopodia and their pockets became part of the intercellular border, other filopodia and their pockets seemed expendable once they functioned to draw opposing membranes together. The length of membrane necessary to seal cell borders is likely to determine this balance. The surface area of membranes encompassed by filopodia and their pockets exceeded this value by a considerable margin.

At more advanced stages of contact, the intercellular border was highly undulated, displaying shallow membranous invaginations lined by AJs (arrows in Figure 7C). These invaginations seemed to be the remnants of utilized filopodia, a prediction consistent with our previously observed merging of two rows of puncta to a single row (see Figure 1C). Moreover, these troughs labeled with antibodies against α-catenin (Figure 7D) and were flanked by desmosomes (De) associated with thick bundles of keratin IFs (Figures 7C and 7D). At late times (~16 hr), the undulating cell–cell border had flattened, and the epithelium appeared as a sheet, with continuous contacts of alternating desmosomes and AJs (Figures 7E and 7G).

In contrast to wild-type keratinocytes, α-catenin null keratinocytes formed few filopodia-like extensions, and

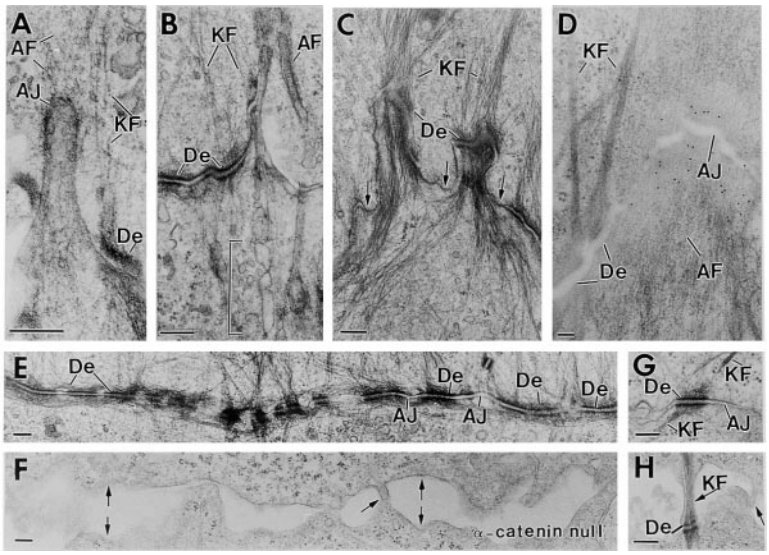

Figure 7. Ultrastructural Analysis of the Fate of Embedded Puncta

At 24 hr after plating, wild-type keratinocytes (A–E and G) or α-E-catenin null keratinocytes (F and H) were treated with calcium for either 4 hr (A–D) or 16 hr (E–H). Cells were then processed for either immunoelectron microscopy with anti-α-catenin (D) or conventional electron microscopy (other frames). Examples in (C) and (D) are of the most mature cell–cell borders found within the sample. Abbreviations: AF, actin filaments; AJ, adherens junction; De, desmosome; KF, keratin filaments. Brackets in (B) denote empty filopodial pockets; arrow in (B) denotes desmosome formed along the side of an embedded, partially relaxed filopodium. Arrows in (C) denote shallow, broad membrane invaginations that contain AJs. These troughs are flanked by desmosomes, and may be filopodial remnants. (D) shows invagination labeled with anti-α-catenin. Double arrows in (F) are of membranes that failed to seal; arrows in (F) and (H) denote short filopodia that have made contact. Bars represent 200 nm.

these did not anchor deeply into the opposing cell's membrane, nor did they organize radial actin fibers (Figures 7F and 7H). Even after 16 hr, large gaps and spaces existed between closely opposed keratinocytes. Occasional desmosomes were still found, but the flanking membranes were not sealed.

Discussion

Filopodia and Active Intercellular Adhesion

The penetration of filopodia as an integral mechanism of intercellular adhesion has not been described, perhaps because the process has been largely studied in immortalized cells that partially crawl over one another at confluence and extend few filopodia. This promiscuity appears to facilitate a process of "passive" adhesion, circumventing the need for filopodia to physically draw neighboring cells sufficiently close to seal their membranes into epithelial sheets.

To what extent is the "active" adhesive process that we describe physiologically relevant? Primary keratinocytes are only a step removed from the tissue itself, and epidermal cells in skin display numerous filopodia-like, interdigitated extensions. A movement-based mechanism for AJ assembly might be especially important where cells are naturally at a distance from each other, such as wound healing or resealing a vacancy after a cell has committed to terminally differentiate and exits the basal layer.

More to Calcium Than Homotypic E-Cadherin Interactions

It has long been recognized that calcium stimulates homotypic engagement of cadherins, which is essential for intercellular adhesion (Nose et al., 1988; Shapiro et al., 1995). Our description of an actin polymerization-based propulsion step in intercellular adhesion expands the role of calcium. While the mechanism is still not clear, it seems likely that calcium activates some key regulatory molecule(s) that in turn leads to actin polymerization at filopodia growth sites (Hall, 1998; Miki et al., 1998; Rohatgi et al., 1999). Although we have not yet investigated whether Cdc42 and N-WASP (or related molecules) are involved in filopodia formation in keratinocytes, these proteins are candidates and could explain

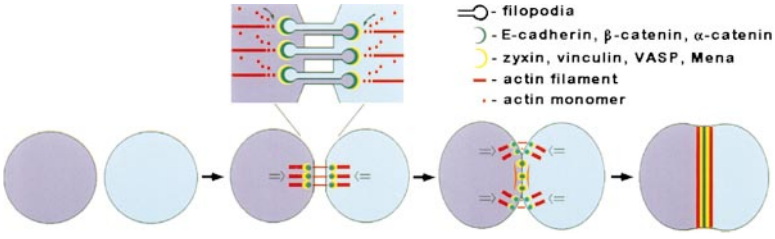

Figure 8. A Model for Adhesion Zipper Function

Two neighboring cells send out filopodia, which upon contact, slide along each other and project into the opposing cell's membrane. Filopodia are rich in F-actin (thin red lines). Embedded tips of filopodia are stabilized by puncta, which are transmembrane clusters of AJ proteins (green crescents). This process draws regions of the two cell surfaces together, which are then clamped by desmosomes. Radial actin fibers (thick red lines) reorganize at filopodia tips in a zyxin-, vinculin-, VASP-, and Mena-dependent fashion (yellow crescents). Actin polymerization is initiated at stabilized puncta (green crescents and dots), creating the directed reverse force needed to push and merge puncta into a single line as new puncta form at edges. The actin-based movement physically brings remaining regions of opposing membranes together and seals them into epithelial sheets. Since filopodia contain actin rather than keratin IFs, they become natural zones of AJs, while the cell surface flanking filopodia becomes fertile ground for desmosome formation, alternating AJs and desmosomes.

the recent report implicating Cdc42 in AJ formation (Kodama et al., 1999).

Puncta, Adhesion Zippers, and Desmosome Formation

The elegant in vitro studies of Nelson and Tsukita and coworkers have given us major insights into AJ formation, identifying puncta as intermediates in the process (McNeill et al., 1993; Yonemura et al., 1995; Adams et al., 1996, 1998; Angres et al., 1996). Our studies reveal the existence of double rows of puncta, and our analysis of adhesion zippers now illuminates how and why puncta form. The penetration of filopodia appears to force opposing cell membranes together, accelerating E-cadherin clustering and AJ formation at the tip to create a punctum. In a dynamic process, an antiparallel pair of filopodia embed into their neighboring cells, physically drawing the two cell surfaces together. Once initial filopodia embed, this anchorage seems to enhance the probability that additional filopodia will make functional contacts, extending the zone of contact between two neighboring cells (see also Drubin and Nelson, 1996).

Desmosomes form in the flanking regions of contact that are brought together by filopodia embedding. In contrast to AJ formation, desmosome assembly seems to be a passive process, with no means to physically bring membranes together, but ready to take advantage of it once stable contact has been made. The stability provided by desmosomes and their anchorage to IF bundles may act as mechanical clamps to preserve the work accomplished by filopodia.

The fact that filopodia are packed primarily with actin rather than IFs sets up a natural zone permissive for AJs but excluding desmosomes. Since desmosomes were the predominant junction at contacts flanking the filopodia, we surmise that desmosome assembly may occur more efficiently than AJ formation whenever two cell surfaces are already in physical contact. Conversely, efficient AJ formation seems to require the force generated by actin-dependent movement. This process quite beautifully explains why desmosomes and AJs alternate at mature cell–cell borders, a phenomenon described by early microscopists, but poorly understood.

Reorganizing the Actin Cytoskeleton and Generating the Force to Seal Membranes Together to Form Epithelial Sheets

Our findings implicate VASP and Mena in actin reorganization and directional polymerization, processes key to epithelial sheet formation. We posit that filopodia-induced clustering of E-cadherin provides the proper conformation and/or density of α-catenin to bind vinculin and/or zyxin and produce a template for subsequent binding of VASP and Mena. While fibroblasts can undergo cell–cell adhesion when they express a recombinant E-cadherin-α-catenin fusion protein lacking the vinculin binding domain of α-catenin (Watabe-Uchida et al., 1998; Imamura et al., 1999), the physiological relevance of that finding is not clear, nor does it exclude a role for zyxin in cell–cell adhesion.

The studies of Laine et al. (1997) suggest that a conformational change in VASP and/or Mena is necessary for them to bind to the family of vinculin/zyxin/Act A proteins. Moreover, recent studies have shown that phosphatidylinositol-4,5-bisphosphate (PIP2) may play an activating role in unmasking vinculin-VASP interaction sites, at least at focal contacts involving integrins (Huttelmaier et al., 1998). Future experiments will be necessary to ascertain whether a similar mechanism is involved at puncta, or whether the physical interaction between vinculin or zyxin and AJ components are alone sufficient to promote VASP/Mena association and activation. Irrespective of mechanism, we speculate that VASP/Mena-dependent reorganization and directed polymerization of actin at stabilized puncta provides the necessary "reverse" force to physically push the two rows of puncta together into a single row and further seal the membranes into an epithelial sheet. A model summarizing these points is presented in Figure 8.

Experimental Procedures

Generation of Epidermal-Specific α-E-Catenin Null Mouse

The details of the generation of these mice were reported (Vasioukhin et al., 1999). They were referred to as Cre-Mate mice, since the nature of the gene targeted for conditional ablation in the epidermis was irrelevant for that study.

Preparation of Primary Keratinocytes

Separation of newborn mouse skin epidermis by dispase, isolation of primary keratinocytes, and culture conditions have been described (Wang et al., 1997). Cells were seeded on glass cover slips (immunofluorescence and scanning EM) or permanox slides (other EM) coated with poly-L-lysine, collagen I, and fibronectin (Collaborative Research, Bedford, MA). MDCK (dog kidney epithelial cells), PtK2 (Potoroo kidney epithelial cells), and UG1 (mouse keratinocytes) were cultured as above. Twenty-four hours after seeding, unattached cells were removed, and AJ formation was induced by increasing the $CaCl_2$ concentration from 0.05 mM to 2 mM.

Immunofluorescence and Electron Microscopy

For immunofluorescence, cells were fixed in 4% formaldehyde in PBS for 10 min, subjected to double indirect immunostaining (Gallicano et al., 1998), and viewed by confocal microscopy (LSM 410 [Carl Zeiss, Thornwood, NY]). Primary antibodies used were against the following: E-cadherin (Zymed, San Francisco, CA), β-catenin (Transduction Laboratories, Lexington, KY), vinculin, α-actinin and phalloidin-TRITC (Sigma, St. Louis, MO), anti-VASP (M4; Alexis, San Diego, CA), anti-Cre (Novagen), anti-WASP (gift from Marc Kirschner, Harvard Medical School), anti-zyxin (gift from Mary Beckerle, University of Utah), anti-Mena (gift from Frank Gertler, MIT), and α-catenin (Sigma, Transduction Laboratories, and gift from Soichiro Tsukita, Kyoto University, Japan). Unless stated, dilutions were according to the manufacturer's recommendations. Fluorescence conjugated secondary antibodies were from ImmunoResearch (West Grove, PA).

Ultrastructural analyses and immunoelectron microscopy were carried out as described (Gallicano et al., 1998). For scanning electron microscopy, cells were fixed with 1.6% formaldehyde and 2.5% glutaraldehyde in PBS, postfixed with 1% osmium tetroxide, and then treated with 0.5% aqueous uranyl acetate. After dehydration in a graded series of ethanol, specimens were dried in hexamethyldisilizane, sputter-coated with gold and viewed with a Joel 840A microscope.

Construction of VASPGFP and Dominant-Negative VASP Expression Plasmids and K14 TD-GFP Transgenic Mice

Human VASP cDNA (I. M. A. G. E clone 824217) was obtained from Genome Systems Inc. Dominant-negative TD-VASP (amino acid residues 277–380; Bachmann et al., 1999) was constructed by PCR amplification with oligonucleotide primers 5′-gcgcctggtaccATGA CGCAAGTTGGGGAGAAAACC-3′ and 5′-gcgcctggatccCAGGGAG

AACCCCGCTTCC-3′. EVH1-VASP was generated in a similar fashion using appropriate oligonucleotide primers (Niebuhr et al., 1997). All cDNAs were ligated into the KpnI and BamHI sites of expression vector pEGFP-N1 (Clontech, Palo Alto, CA). PCR-generated sequences were verified by sequencing. Primary keratinocytes were transfected using Fugene 6 reagent (Roche, Indianapolis, IN).

TDGFP was inserted into the BamH1 site of the K14 cassette, and transgenic mice were engineered as described (Wang et al., 1997). Five transgenic mice were generated that expressed the transgene in the epidermis as judged by green fluorescence. We present data on the mouse whose skin most intensely and uniformly fluoresced.

Peptide Microinjections

Pure custom-made peptide CFEFPPPPTDE (Zymed, San Francisco, CA) was diluted in microinjection buffer containg 10 mM Tris-HCl, pH 7.2, and 2 mg/ml of Texas red–conjugated, lysinated dextran (Molecular Probes, Eugene, OR). Groups of cells were microinjected with 1–10 μM of peptide using a micromanipulator, microinjector, and femtotip II (Eppendorf, Westbury, NY). Control cells were microinjected with buffer alone. At 30 min following microinjection, AJs were induced by calcium.

Acknowledgments

We thank Dr. S. Tsukita for anti-α-catenin and cDNA, Dr. M. Beckerle for anti-zyxin, Dr. F. Gertler for anti-Mena, Dr. M. Kirschner for anti-N-WASP, Dr. E. Williamson and Dr. Q. C. Yu for their assistance in electron microscopy, and Linda Degenstein for her assistance with mice. This work was supported by grants from the National Institutes of Health (R01-AR27883) and the National Cancer Institute (5P50 DE11921). E. F. is an Investigator of the Howard Hughes Medical Institute.

Received October 19, 1999; revised December 17, 1999.

References

Adams, C.L., Nelson, W.J., and Smith, S.J. (1996). Quantitative analysis of cadherin-catenin-actin reorganization during development of cell–cell adhesion. J. Cell Biol. *135*, 1899–1911.

Adams, C.L., Chen, Y.T., Smith, S.J., and Nelson, W.J. (1998). Mechanisms of epithelial cell–cell adhesion and cell compaction revealed by high-resolution tracking of E-cadherin-green fluorescent protein. J. Cell Biol. *142*, 1105–1119.

Angres, B., Barth, A., and Nelson, W.J. (1996). Mechanism for transition from initial to stable cell–cell adhesion: kinetic analysis of E-cadherin-mediated adhesion using a quantitative adhesion assay. J. Cell Biol. *134*, 549–557.

Bachmann, C., Fischer, L., Walter, U., and Reinhard, M. (1999). The EVH2 domain of the vasodilator-stimulated phosphoprotein mediates tetramerization, F-actin binding, and actin bundle formation. J. Biol. Chem. *274*, 23549–23557.

Beckerle, M.C. (1998). Spatial control of actin filament assembly: lessons from Listeria. Cell *95*, 841–748.

Bershadsky, A., and Geiger, B. (1998). Anchor and adhesion proteins. In Guidebook to the Extracellular Matrix, T. Kreis and R. Vale, eds. (Oxford, England: Oxford University Press), pp. 3–14.

Braga, V.M., Machesky, L.M., Hall, A., and Hotchin, N.A. (1997). The small GTPases Rho and Rac are required for the establishment of cadherin-dependent cell–cell contacts. J. Cell Biol. *137*, 1421–1431.

Braga, V.M., Del Maschio, A., Machesky, L., and Dejana, E. (1999). Regulation of cadherin function by Rho and Rac: modulation by junction maturation and cellular context. Mol. Biol. Cell *10*, 9–22.

Drubin, D.G., and Nelson, W.J. (1996). Origins of cell polarity. Cell *84*, 335–344.

Gallicano, I.G., Kouklis, P., Bauer, C., Yin, M., Vasioukhin, V., Degenstein, L., and Fuchs, E. (1998). Desmoplakin is required early in development for assembly of desmosomes and cytoskeletal linkage. J. Cell Biol. *143*, 2009–2022.

Geiger, B., Ayalon, O., Ginsberg, D., Volberg, T., Rodriguez Fernandez, J.L., Yarden, Y., and Ben-Ze'ev, A. (1992). Cytoplasmic control of cell adhesion. Cold Spring Harb. Symp. Quant. Biol. *57*, 631–642.

Gumbiner, B.M. (1996). Cell adhesion: the molecular basis of tissue architecture and morphogenesis. Cell *84*, 345–357.

Hall, A. (1998). Rho GTPases and the actin cytoskeleton. Science *279*, 509–514.

Hazan, R.B., Kang, L., Roe, S., Borgen, P.I., and Rimm, D.L. (1997). Vinculin is associated with the E-cadherin adhesion complex. J. Biol. Chem. *272*, 32448–32453.

Huttelmaier, S., Mayboroda, O., Harbeck, B., Jarchau, T., Jockusch, B.M., and Rudiger, M. (1998). The interaction of the cell-contact proteins VASP and vinculin is regulated by phosphatidylinositol-4, 5-bisphosphate. Curr. Biol. *8*, 479–488.

Imamura, Y., Itoh, M., Maeno, Y., Tsukita, S., and Nagafuchi, A. (1999). Functional domains of alpha-catenin required for the strong state of cadherin-based cell adhesion. J. Cell Biol. *144*, 1311–1322.

Knudsen, K.A., Soler, A.P., Johnson, K.R., and Wheelock, M.J. (1995). Interaction of α-actinin with the cadherin/catenin cell–cell adhesion complex via α-catenin. J. Cell Biol. *130*, 67–77.

Kodama, A., Takaishi, K., Nakano, K., Nishioka, H., and Takai, Y. (1999). Involvement of Cdc42 small G protein in cell–cell adhesion, migration and morphology of MDCK cells. Oncogene *18*, 3996–4006.

Kowalczyk, A.P., Bornslaeger, E.A., Norvell, S.M., Palka , H.L., and Green, K.J. (1999). Desmosomes: intercellular adhesive junctions specialized for attachment of intermediate filaments. Int. Rev. Cytol. *185*, 237–302.

Kuroda, S., Fukata, M., Fujii, K., Nakamura, T., Izawa, I., and Kaibuchi, K. (1997). Regulation of cell–cell adhesion of MDCK cells by Cdc42 and Rac1 small GTPases. Biochem. Biophys. Res. Commun. *240*, 430–435.

Laine, R.O., Zeile, W., Kang, F., Purich, D.L., and Southwick, F.S. (1997). Vinculin proteolysis unmasks an ActA homolog for actin-based Shigella motility. J. Cell Biol. *138*, 1255–1264.

Lau, P.M., Zucker, R.S., and Bentley, D. (1999). Induction of filopodia by direct local elevation of intracellular calcium ion concentration. J. Cell Biol. *145*, 1265–1275.

Laurent, V., Loisel, T.P., Harbeck, B., Wehman, A., Grobe, L., Jockusch, B.M., Wehland, J., Gertler, F.B., and Carlier, M.F. (1999). Role of proteins of the Ena/VASP family in actin-based motility of Listeria monocytogenes. J. Cell Biol. *144*, 1245–1258.

Machesky, L.M., and Insall, R.H. (1999). Signaling to actin dynamics. J. Cell Biol. *146*, 267–272.

McNeill, H., Ryan, T.A., Smith, S.J., and Nelson, W.J. (1993). Spatial and temporal dissection of immediate and early events following cadherin-mediated epithelial cell adhesion. J. Cell Biol. *120*, 1217–1226.

Miki, H., Sasaki, T., Takai, Y., and Takenawa, T. (1998). Induction of filopodium formation by a WASP-related actin-depolymerizing protein N-WASP. Nature *391*, 93–96.

Niebuhr, K., Ebel, F., Frank, R., Reinhard, M., Domann, E., Carl, U.D., Walter, U., Gertler, F.B., Wehland, J., and Chakraborty, T. (1997). A novel proline-rich motif present in ActA of Listeria monocytogenes and cytoskeletal proteins is the ligand for the EVH1 domain, a protein module present in the Ena/VASP family. EMBO J. *16*, 5433–5444.

Nose, A., Nagafuchi, A., and Takeichi, M. (1988). Expressed recombinant cadherins mediate cell sorting in model systems. Cell *54*, 993–1001.

Reinhard, M., Halbrugge, M., Scheer, U., Wiegand, C., Jockusch, B.M., and Walter, U. (1992). The 46/50 kDa phosphoprotein VASP purified from human platelets is a novel protein associated with actin filaments and focal contacts. EMBO J. *11*, 2063–2070.

Reinhard, M., Zumbrunn, J., Jaquemar, D., Kuhn, M., Walter, U., and Trueb, B. (1999). An alpha-actinin binding site of zyxin is essential for subcellular zyxin localization and alpha-actinin recruitment. J. Biol. Chem. *274*, 13410–13418.

Rohatgi, R., Ma, L., Miki, H., Lopez, M., Kirchhausen, T., Takenawa, T., and Kirschner, M.W. (1999). The interaction between N-WASP and the Arp2/3 complex links Cdc42-dependent signals to actin assembly. Cell *97*, 221–231.

Shapiro, L., Fannon, A.M., Kwong, P.D., Thompson, A., Lehmann, M.S., Grubel, G., Legrand, J.F., Als-Nielsen, J., Colman, D.R., and Hendrickson, W.A. (1995). Structural basis of cell–cell adhesion by cadherins. Nature *374*, 327–337.

Southwick, F.S., and Purich, D.L. (1994). Arrest of Listeria movement in host cells by a bacterial ActA analogue: implications for actin-based motility. Proc. Natl. Acad. Sci. USA *91*, 5168–5172.

Symons, M.H., and Mitchison, T.J. (1991). Control of actin polymerization in live and permeabilized fibroblasts. J. Cell Biol. *114*, 503–513.

Stoffler, H.E., Honnert, U., Bauer, C.A., Hofer, D., Schwarz, H., Muller, R.T., Drenckhahn, D., and Bahler, M. (1998). Targeting of the myosin-I myr 3 to intercellular adherens type junctions induced by dominant active Cdc42 in HeLa cells. J. Cell Sci. *111*, 2779–2788.

Vasioukhin, V., Degenstein, L., Wise, B., and Fuchs, E. (1999). The magical touch: genome targeting in epidermal stem cells induced by tamoxifen application to mouse skin. Proc. Natl. Acad. Sci. USA *96*, 8551–8556.

Wang, X., Zinkel, S., Polansky, K., and Fuchs, E. (1997). Marked growth enhancement in transgenic mice expressing keratin promoter-driven human growth hormone: implications for keratinocyte mediated gene therapy. Proc. Natl. Acad. Sci. USA *94*, 219–226.

Watabe-Uchida, M., Uchida, N., Imamura, Y., Nagafuchi, A., Fujimoto, K., Uemura, T., Vermeulen, S., van Roy, F., Adamson, E.D., et al. (1998). Alpha-catenin-vinculin interaction functions to organize the apical junctional complex in epithelial cells. J. Cell Biol. *142*, 847–857.

Yonemura, S., Itoh, M., Nagafuchi, A., and Tsukita, S. (1995). Cell-to-cell adherens junction formation and actin filament organization: similarities and differences between non-polarized fibroblasts and polarized epithelial cells. J. Cell Sci. *108*, 127–142.